

Electronic Supplementary Information (ESI)

1. General information

All the chemicals and reagents were purchased from commercial sources and used for reaction without further purification. The final products were collected via silica-gel column chromatography and further purified by vacuum sublimation. ^1H NMR and ^{13}C NMR spectrums were obtained based on a Bruker AV 400 or 500 spectrometer in CDCl_3 , CD_2Cl_2 or $\text{DMSO-}d_6$ solvent. High-resolution mass spectra (HRMS) were tested on Agilent1290/Bruker maXis impact. Single-crystals were obtained in THF/hexane or chloroform/hexane systems via slow solvent evaporation, and were analyzed on a Bruker–Nonices Smart Apex CCD diffractometer with graphite monochromated $\text{MoK}\alpha$ radiation. UV-vis absorption spectra were collected on Shimadzu UV-2600 spectrophotometer. Photoluminescence (PL) spectra were measured on a Horiba Fluoromax-4 spectrofluorometer. PL quantum yields were obtained on Hamamatsu absolute PL quantum yield spectrometer C11347 Quantaaurus_QY. Thermal decomposition temperatures (T_{ds}) were gathered on a NETZSCH STA449F5 at a heating rate of $10\text{ }^\circ\text{C min}^{-1}$. Cyclic voltammogram was characterized in dichloromethane or *N,N*-dimethylformamide using tetra-*n*-butylammonium hexafluorophosphate (Bu_4NPF_6 , 0.1 M) as supporting electrolyte at a scan rate of 0.1 V s^{-1} . Glassy carbon, platinum wire and Ag/Ag^+ electrode were employed as work, counter and reference electrode, respectively. The energy levels of highest occupied molecular orbitals (HOMOs) were calculated from the equation: $\text{HOMO} = -(E_{\text{onset}}^{\text{ox}} - E_{\text{Fc}/\text{Fc}^+}^{\text{ox}} + 4.8)\text{ eV}$, and those of the lowest unoccupied molecular orbitals (LUMOs) were calculated from the equation: $\text{LUMO} = -(E_{\text{onset}}^{\text{red}} - E_{\text{Fc}/\text{Fc}^+}^{\text{red}} + 4.8)\text{ eV}$. The ground-state geometries were optimized based on density functional theory (DFT) method at the B3LYP/6-31G (d,p) level. All the calculations were performed using Gaussian 09 or Gaussian 16 package.

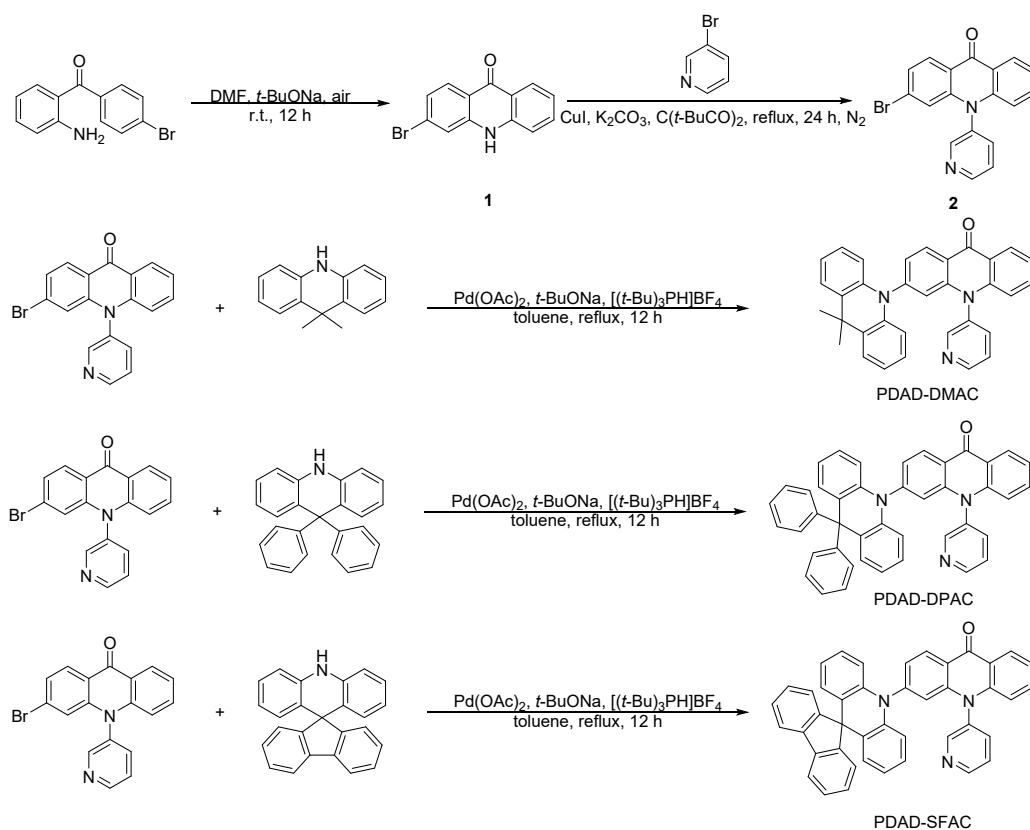
2. Fabrication and characterization for OLEDs

Glass substrates pre-coated with a 90-nm-thin layer of indium tin oxide (ITO) with a sheet resistance of $15\sim 20\ \Omega$ per square were completely cleaned in ultrasonic bath followed by washing acetone, isopropanol, detergent and deionized water, and each step takes 10 minutes. After that, the substrates were dried totally in a $70\text{ }^\circ\text{C}$ oven and treated by O_2 plasma for 10 minutes to enhance the hole-

injection ability of ITO. The vacuum-deposited OLEDs were fabricated with Fangsheng OMV-FS450 vacuum deposition system under a pressure of $< 5 \times 10^{-4}$ Pa. Organic materials, LiF and Al were deposited at rates of $1\sim 2 \text{ \AA s}^{-1}$, 0.1 \AA s^{-1} and 5 \AA s^{-1} , respectively.

The luminance–voltage–current density curves and electroluminescence (EL) spectra were gained using a Konica Minolta CS-200 Color and Luminance Meter and an Ocean Optics USB 2000+ spectrometer, along with a Keithley 2400 Source Meter. The external quantum efficiencies were calculated via current efficiencies and normalized EL spectra of devices, assuming that the devices are Lambertian emitters. The effective emitting area of the device was 9 mm^2 , determined by the overlap between anode and cathode. All the characterizations were done at room temperature in ambient conditions without extra encapsulation.

3. Syntheses and characterization



Scheme S1. Synthetic routes of the new molecules.

3-Bromoacridin-9(10H)-one (1): 2-Amino-4'-bromobenzophenone (5.52 g, 20.0 mmol), sodium *tert*-butoxide (3.84 g, 40.0 mmol) and *N,N*-dimethylformamid (DMF, 100 mL) were added to a two-neck flask. The mixture was stirred at room temperature for 12 h under air atmosphere. Then, the reaction mixture was poured into a lot of water and lots of solid was precipitated. The solid was

washed with water and then ethanol, and dried under vacuum (40 °C). 3-Bromoacridin-9(10H)-one was obtained as yellow solid in 52% yield. ¹H NMR (500 MHz, DMSO-*d*₆), δ (ppm): 11.80 (s, 1H), 8.23–8.21 (m, 1H), 8.14 (d, *J* = 8.6 Hz, 1H), 7.78–7.75 (m, 1H), 7.72 (d, *J* = 1.8 Hz, 1H), 7.53 (d, *J* = 8.3 Hz, 1H), 7.41–7.39 (m, 1H), 7.32–7.27 (m, 1H). ¹³C NMR (125 MHz, DMSO-*d*₆), δ (ppm): 176.83, 142.19, 141.24, 134.38, 128.83, 127.56, 126.49, 124.56, 122.11, 121.15, 119.88, 119.83, 117.96. HRMS: *m/z* [M⁺] calcd for C₁₃H₈BrNO, 272.9789; found, 272.9826.

3-Bromo-10-(pyridin-3-yl)acridin-9(10H)-one (2): A mixture of **1** (2.74 g, 10.0 mmol), 3-bromopyridine (2.37 g, 15.0 mmol), copper(I) iodide (0.19 g, 1.0 mmol), K₂CO₃ (2.07 g, 15.0 mmol), and 2,2,6,6-tetramethyl-3,5-heptanedione (0.37 g, 2.0 mmol) were mixed in DMF (80 mL) under nitrogen. The mixture was heated to reflux for 24 h. After cooling to room temperature, the mixture was poured into a large amount of water and extracted with dichloromethane. The combined organic layers were washed with water for three times and dried over anhydrous MgSO₄. After filtration and solvent evaporation, the residue was purified by alumina column chromatography using dichloromethane/petroleum ether as an eluent. 3-Bromo-10-(pyridin-3-yl)acridin-9(10H)-one was obtained as yellow solid in 10% yield. ¹H NMR (500 MHz, CDCl₃), δ (ppm): 8.98 (d, *J* = 3.4 Hz, 1H), 8.70 (s, 1H), 8.57–8.55 (m, 1H), 8.44 (d, *J* = 8.6 Hz, 1H), 7.82–7.79 (m, 1H), 7.76–7.73 (m, 1H), 7.56–7.53 (m, 1H), 7.43–7.41 (m, 1H), 7.36–7.32 (m, 1H), 6.81 (d, *J* = 1.6 Hz, 1H), 6.64 (d, *J* = 8.6 Hz, 1H). ¹³C NMR (125 MHz, CDCl₃), δ (ppm): 177.42, 151.36, 151.08, 143.63, 142.97, 138.25, 135.30, 133.97, 129.36, 128.83, 127.65, 125.78, 125.63, 122.61, 122.10, 120.71, 118.82, 116.37. HRMS: *m/z* [M⁺] calcd for C₁₈H₁₁BrN₂O, 350.0055; found, 350.0098.

9',9'-Dimethyl-10-(pyridin-3-yl)-9'H-[3,10'-biacridin]-9(10H)-one (PDAD-DMAC): A mixture of **2** (0.35 g, 1.0 mmol), 9,9-dimethyl-9,10-dihydro-acridine (0.25 g, 1.2 mmol), palladium diacetate (0.023 g, 0.1 mmol), tri-*tert*-butylphosphine tetrafluoroborate (0.029 g, 0.1 mmol) and sodium *tert*-butoxide (0.19 g, 2.0 mmol) were stirred and refluxed in toluene (30 mL) for 12 h under nitrogen. After cooling to room temperature, the reaction mixture was poured into water and extracted with dichloromethane. The combined organic layers were washed with water, and dried with MgSO₄. The crude product was purified by alumina column chromatography using dichloromethane/petroleum ether as eluent. PDAD-DMAC was obtained as a green solid in 75% yield. ¹H NMR (400 MHz, DMSO-*d*₆), δ (ppm): 8.82 (s, 2H), 8.64 (d, *J* = 8.5 Hz, 1H), 8.44 (d, *J* = 7.6 Hz, 1H), 8.16 (d, *J* = 8.0 Hz, 1H), 7.77–7.74 (m, 1H), 7.72–7.67 (m, 1H), 7.47 (d, *J* = 6.7 Hz, 2H), 7.44–7.39 (m, 1H), 7.28 (d,

$J = 8.3$ Hz, 1H), 7.01–6.90 (m, 4H), 6.73 (d, $J = 8.6$ Hz, 1H), 6.58 (s, 1H), 6.32 (d, $J = 7.6$ Hz, 2H), 1.53 (s, 6H). ^{13}C NMR (125 MHz, DMSO- d_6), δ (ppm): 176.76, 151.41, 151.39, 146.31, 145.25, 143.44, 140.12, 138.76, 135.50, 134.76, 131.68, 130.46, 127.01, 126.97, 126.42, 125.90, 123.02, 122.82, 121.97, 121.91, 120.57, 117.32, 117.28, 115.35, 36.20, 31.15. HRMS: m/z [M^+] calcd for $\text{C}_{33}\text{H}_{25}\text{N}_3\text{O}$, 479.1998; found, 479.2079.

9',9'-Diphenyl-10-(pyridin-3-yl)-9'H-[3,10'-biacridin]-9(10H)-one (PDAD-DPAC): The target product was obtained using **2** (0.35 g, 1.0 mmol), 9,9-diphenyl-9,10-dihydroacridine (0.40 g, 1.2 mmol), palladium diacetate (0.023 g, 0.1 mmol), tri-*tert*-butylphosphine tetrafluoroborate (0.029 g, 0.1 mmol) and sodium *tert*-butoxide (0.19 g, 2.0 mmol) following the procedure described for PDAD-DMAC. Green solid, yield: 72%. ^1H NMR (400 MHz, CDCl_3), δ (ppm): 8.87–8.86 (m, 1H), 8.70 (d, $J = 8.5$ Hz, 1H), 8.64–8.56 (m, 2H), 7.68–7.64 (m, 1H), 7.59–7.50 (m, 2H), 7.37–7.32 (m, 1H), 7.23–7.11 (m, 6H), 7.10–7.01 (m, 3H), 6.96–6.81 (m, 8H), 6.62 (d, $J = 8.5$ Hz, 1H), 6.45 (d, $J = 7.9$ Hz, 2H), 6.28 (d, $J = 1.7$ Hz, 1H). ^{13}C NMR (125 MHz, CD_2Cl_2), δ (ppm): 178.23, 150.37, 149.79, 147.45, 147.13, 145.95, 144.29, 142.79, 141.94, 137.49, 135.18, 132.61, 131.55, 131.22, 128.88, 128.71, 128.21, 127.92, 127.71, 124.99, 123.88, 123.50, 122.35, 122.21, 117.77, 117.59, 116.30, 58.18. HRMS: m/z [M^+] calcd for $\text{C}_{43}\text{H}_{29}\text{N}_3\text{O}$, 603.2311; found, 603.2378.

10-(Pyridin-3-yl)-3-(10H-spiro[acridine-9,9'-fluoren]-10-yl)acridin-9(10H)-one (PDAD-SFAC): The target product was obtained using **2** (0.35 g, 1.0 mmol), 9,9-diphenyl-9,10-dihydroacridine (0.40 g, 1.2 mmol), palladium diacetate (0.023 g, 0.1 mmol), tri-*tert*-butylphosphine tetrafluoroborate (0.029 g, 0.1 mmol) and sodium *tert*-butoxide (0.19 g, 2.0 mmol) following the procedure described for PDAD-DMAC. Green solid, yield: 73%. ^1H NMR (400 MHz, CD_2Cl_2), δ (ppm): 8.80 (d, $J = 8.3$ Hz, 2H), 8.66 (s, 1H), 8.54–8.49 (m, 1H), 7.80 (d, $J = 8.1$ Hz, 1H), 7.73 (d, $J = 7.6$ Hz, 2H), 7.64–7.59 (m, 1H), 7.55–7.49 (m, 1H), 7.36–7.27 (m, 4H), 7.21–7.11 (m, 4H), 6.85–6.81 (m, 3H), 6.66 (d, $J = 8.6$ Hz, 1H), 6.49–6.44 (m, 2H), 6.28–6.22 (m, 4H). ^{13}C NMR (100 MHz, CD_2Cl_2), δ (ppm): 177.20, 156.25, 150.96, 150.65, 145.94, 145.16, 143.32, 140.68, 139.22, 138.41, 135.53, 133.93, 130.92, 128.31, 127.75, 127.56, 127.36, 127.33, 125.94, 125.41, 124.91, 124.56, 122.51, 122.27, 121.70, 120.84, 120.07, 118.97, 116.66, 114.62, 56.63. HRMS: m/z [M^+] calcd for $\text{C}_{43}\text{H}_{27}\text{N}_3\text{O}$, 601.2154; found, 601.2208.

4. X-Ray crystallography

Crystal data for PDAD-DMAC (CCDC 2053968): $C_{33}H_{25}N_3O$, $M_W = 479.56$, triclinic, P-1, $a = 13.6487(8)$, $b = 14.1942(8)$, $c = 15.4278(10)$ Å, $\alpha = 90.730(2)^\circ$, $\beta = 113.037(2)^\circ$, $\gamma = 113.915(2)^\circ$, $V = 2461.6(3)$ Å³, $Z = 4$, $D_c = 1.294$ g cm⁻³, $\mu = 0.079$ mm⁻¹ (MoK α , $\lambda = 0.71073$), $F(000) = 1008$, $T = 173(2)$ K, $2\theta_{\max} = 25.397^\circ$ (96.5%), 17983 measured reflections, 8759 independent reflections ($R_{\text{int}} = 0.0776$), GOF on $F^2 = 1.059$, $R_1 = 0.1657$, $wR_2 = 0.1499$ (all data), Δe 0.157 and -0.204 eÅ⁻³.

Crystal data for PDAD-DPAC (CCDC: 2053971): $C_{43}H_{29}N_3O$, $M_W = 603.69$, triclinic, P-1, $a = 10.7981(7)$, $b = 12.3945(7)$, $c = 12.6081(7)$ Å, $\alpha = 88.636(2)^\circ$, $\beta = 74.521(2)^\circ$, $\gamma = 66.783(2)^\circ$, $V = 1488.21(15)$ Å³, $Z = 2$, $D_c = 1.347$ g cm⁻³, $\mu = 0.081$ mm⁻¹ (MoK α , $\lambda = 0.71073$), $F(000) = 632$, $T = 173(2)$ K, $2\theta_{\max} = 25.024^\circ$ (97.3%), 16014 measured reflections, 5103 independent reflections ($R_{\text{int}} = 0.0503$), GOF on $F^2 = 1.035$, $R_1 = 0.0792$, $wR_2 = 0.1099$ (all data), Δe 0.249 and -0.174 eÅ⁻³.

Crystal data for PDAD-SFAC (CCDC: 2053969): $C_{43}H_{27}N_3O$, $M_W = 639.19$, triclinic, P-1, $a = 9.4967(4)$, $b = 19.9207(9)$, $c = 20.1366(8)$ Å, $\alpha = 78.942(2)^\circ$, $\beta = 86.2920(10)^\circ$, $\gamma = 79.882(2)^\circ$, $V = 3678.7(3)$ Å³, $Z = 4$, $D_c = 1.154$ g cm⁻³, $\mu = 0.135$ mm⁻¹ (MoK α , $\lambda = 0.71073$), $F(000) = 1329$, $T = 173(2)$ K, $2\theta_{\max} = 23.302$ (97.1%), 32306 measured reflections, 10330 independent reflections ($R_{\text{int}} = 0.0863$), GOF on $F^2 = 1.192$, $R_1 = 0.1780$, $wR_2 = 0.2934$ (all data), Δe 0.898 and -0.407 eÅ⁻³.

5. Additional data

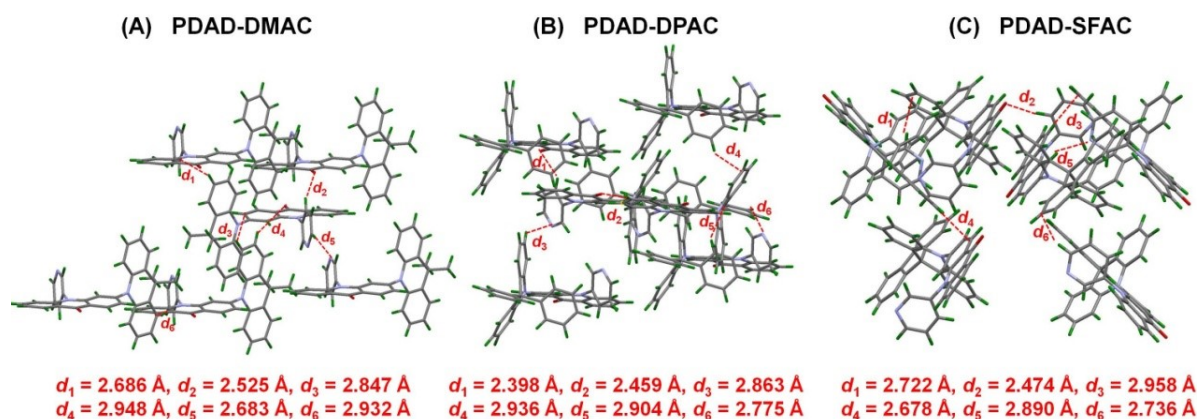


Fig. S1 Molecular packing models and intermolecular interactions of PDAD-DMAC, PDAD-DPAC and PDAD-SFAC.

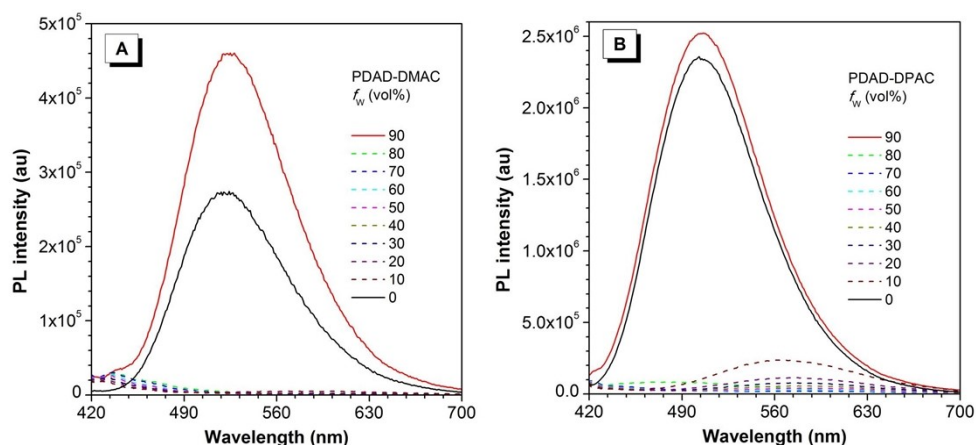


Fig. S2 PL spectra of (A) PDAD-DMAC and (B) PDAD-DPAC in THF/water mixtures with different water fractions (f_w vol%) (concentration = 10^{-5} M).

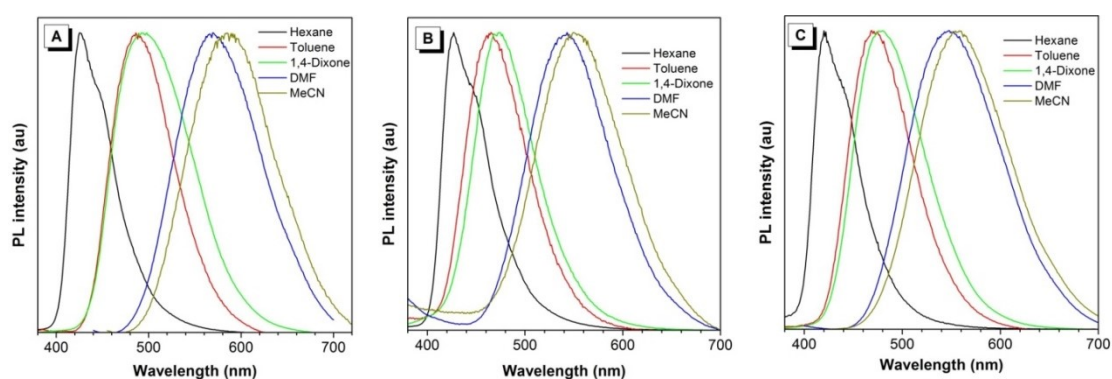


Fig. S3 PL spectra of (A) PDAD-DMAC, (B) PDAD-DPAC and (C) PDAD-SFAC in different solvents (concentration = 10^{-5} M).

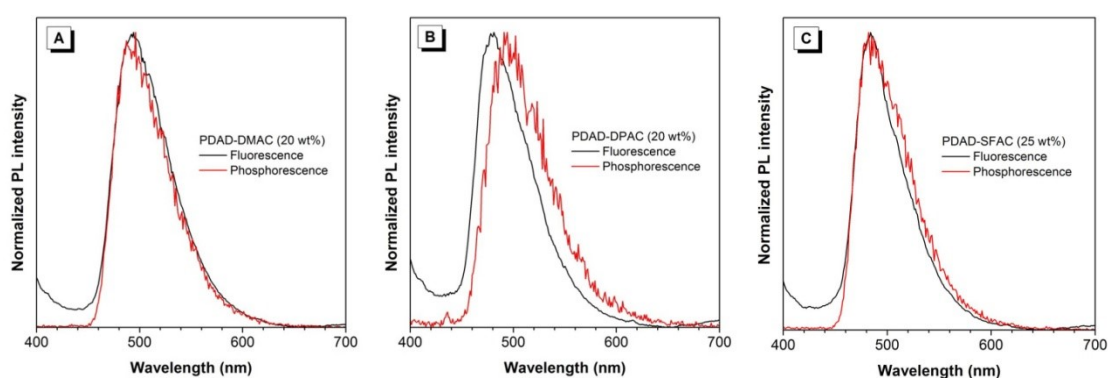


Fig. S4 Fluorescence and phosphorescence spectra of (A) PDAD-DMAC and (B) PDAD-DPAC and (C) PDAD-SFAC in doped films measured under nitrogen at 77 K.

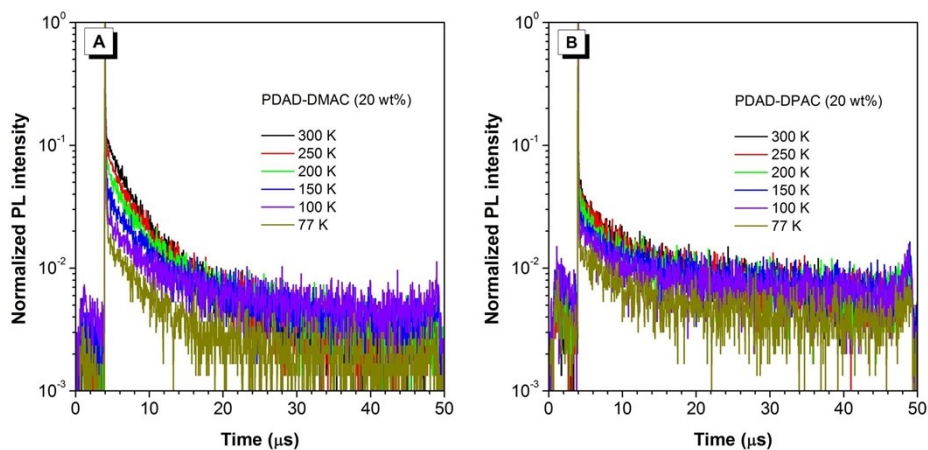


Fig. S5 Temperature-dependent transient PL decay spectra of doped films under nitrogen.

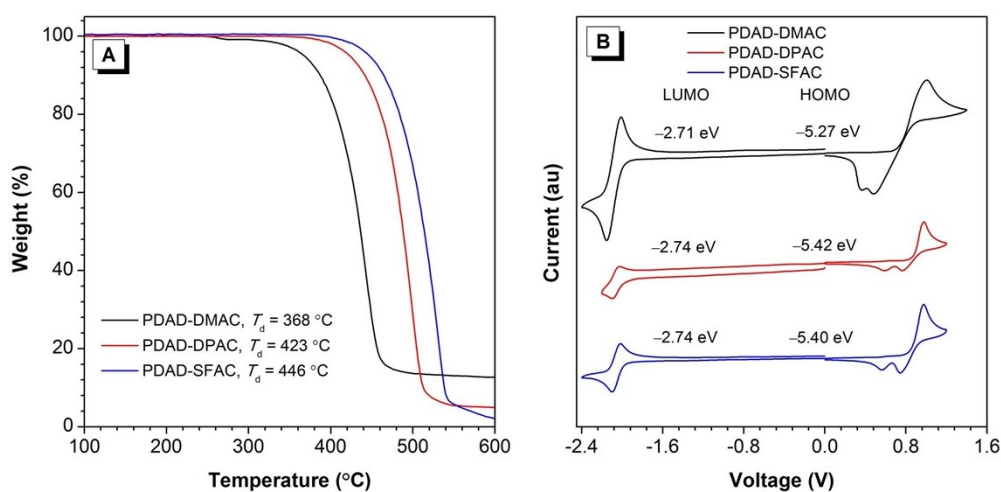


Fig. S6 (A) Thermogravimetric analysis (TGA) spectra, measured at a heating rate of $10\text{ }^{\circ}\text{C min}^{-1}$. (B) Cyclic voltammograms, recorded at a scanning rate of 0.1 V s^{-1} .

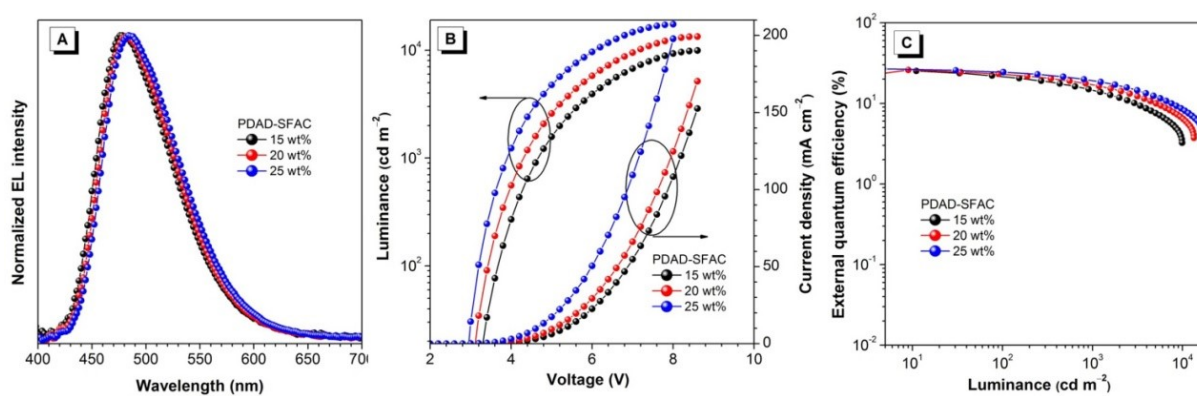


Fig. S7 (A) EL spectra, (B) luminance–voltage–current density curves and (C) external quantum efficiency–luminance curves of PDAD-SFAC at different doped concentrations.

Table S1. EL performances of PDAD-SFAC at different doping concentrations.^a

PDAD-SFAC	V_{on} (V)	L_{max} (cd m^{-2})	$\eta_{\text{C,max}}$ (cd A^{-1})	$\eta_{\text{P,max}}$ (lm W^{-1})	$\eta_{\text{ext,max}}$ (%)	CIE (x, y)	λ_{EL} (nm)
15 wt%	3.1	9917	50.4	49.5	25.3	(0.169, 0.337)	476
20 wt%	2.9	13381	54.4	57.0	25.9	(0.179, 0.362)	484
25 wt%	2.7	17393	59.2	66.4	26.8	(0.181, 0.386)	484

^a V_{on} = turn on voltage at 1 cd m^{-2} ; L_{max} = maximum luminance; $\eta_{\text{C,max}}$ = maximum current efficiency; $\eta_{\text{P,max}}$ = maximum power efficiency; $\eta_{\text{ext,max}}$ = maximum external quantum efficiency; CIE = Commission Internationale de l'Eclairage coordinates; λ_{EL} = EL peak. Device configuration: ITO/HATCN (5 nm)/TAPC (50 nm)/TcTa (5 nm)/mCP (5 nm)/PDAD-SFAC: PPF (x wt%, 20 nm)/PPF (5 nm)/TmPyPB (30 nm)/LiF (1 nm)/Al, where x is 15, 20 and 25, respectively.